MODIFIED MODEL FOR THERMOELECTRIC GENERATORS

Michael Freunek, Leonhard M. Reindl, William D. Walker

Laboratory of Electrical Instrumentation, Department of Microsystems Engineering (IMTEK), Albert-Ludwigs-Universität Freiburg, D-79110
michael.freunek@imtek.uni-freiburg.de, Phone: +49 (0)761-203-7225

Abstract

In this paper we describe a modified analytical model for thermoelectric generators (TEG). The model includes the Peltier heat, a parameterization of the Joule heat, as well as all thermal and electrical resistances. Geometry optimization and investigations of the influence of Peltier heat and the heat sink conditions, which affect the power output, is presented. The results are compared with measurements of commercially available thermo-electric generators and the fundamental thermodynamic limit. A comparison between the generators is performed.

Introduction

TEGs convert heat energy into electrical power, where charge carriers serve as the working fluid. TEGs have many attractive features, like no moving parts, little maintenance, and can be designed in a number of shapes for many specific applications. TEGs can be used to power autonomous sensors and play an important part for energy harvesting systems. To use the provided heat energy in the best way, the determination of the optimal thermo-electric-system geometry, as well as an appropriate thermoelectric material selection, is of particular interest. To that end, a sophisticated generator model, relating the power output to the system parameters is necessary. Furthermore, such a model improves the predictive power of convertible heat energy, which is one of the major drawbacks in designing energy harvesting systems powered by heat energy.

TEG Model Calculation

The basic physical effects taking place in a TEG (Figure 1) are thermal conduction, the Seebeck, Peltier, Thompson and Joule-effect. Neglecting temperature dependences of all physical properties, according to the Thomson effect, the basic TEG equations can be written as follows [1]:

$$U_0 = m\alpha\Delta T_g \tag{1}$$

$$I = \frac{U_0}{R_l + R_g} \tag{2}$$

$$P_{out} = (U_0)^2 \frac{R_l}{(R_l + R_g)^2} \tag{3}$$

$$P_{Joule} = (U_0)^2 \frac{R_g}{(R_l + R_g)^2} \tag{4}$$

$$q_h = \frac{\Delta T_g}{K_g} + IT_h\alpha - \frac{1}{2}I^2R - I^2R_{ch} \tag{5}$$

$$q_c = \frac{\Delta T_g}{K_g} + IT_c\alpha + \frac{1}{2}I^2R + I^2R_{cc} \tag{6}$$

$$R_g = R + R_{ch} + R_{cc} \tag{7}$$

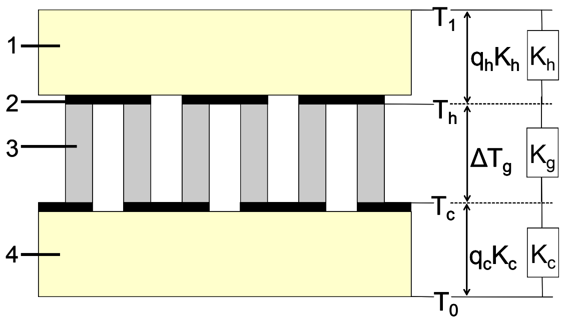

FIGURE 1: Thermoelectric generator. 1: thermal resistance of wafer and contact to the heat source; 2: conducting strip; 3: thermo legs; 4: thermal resistance of wafer and cooler and contact to the heat sink.

U_0 describes the TEG voltage, α the Seebeck coefficient, m the number of thermocouples, $\Delta T_g = T_h - T_c$ the temperature difference at the thermo-couples, R_l the load resistance, I the electric current, q_h and q_c the heat flux between the electrical junctions and the heat source and heat sink. K_g is the thermal resistance of the thermocouples, K_h and K_c are the thermal resistances between the thermocouples and the heat source, heat sink, respectively. The inner resistance R_g is the sum of the resistance R of the thermocouples and the contact resistances R_{ch} and R_{cc} at the hot- and cold side [1]. Introducing the parameter ε

$$\varepsilon = \frac{\frac{1}{2}R + R_{cc}}{R + R_{cc} + R_{ch}}, \tag{8}$$

equation (5) and (6) can be rewritten in the following way:

$$q_h = \frac{\Delta T_g}{K_g} + IT_h\alpha - (1-\varepsilon)P_{Joule} \tag{9}$$

$$q_c = \frac{\Delta T_g}{K_g} + IT_c\alpha + \varepsilon P_{Joule} \tag{10}$$

The temperature difference ΔT_g dropped at the thermo couples is affected by the thermal resistances, the Peltier effect and the Joule heat, which is smaller than $\Delta T = T_1 - T_0$, the temperature difference applied to the TEG. The relationship between ΔT_g and ΔT is shown in the following equation:

$$\Delta T = \Delta T_g + K_c q_c + K_h q_h \tag{11}$$

Combining equation (1,2, 9-11), q_h and q_c become:

$$q_h = \frac{R_l + R_g}{R_l + R_g + (m\alpha)^2 K_h \Delta T_g} \cdot \left(\frac{\Delta T_g}{K_g} + \frac{(m\alpha)^2 T_1 \Delta T_g}{R_l + R_g} - (1-\varepsilon)\left(m\alpha\Delta T_g\right)^2 \frac{R_l}{\left(R_l + R_g\right)^2} \right) \tag{12}$$

$$q_c = \frac{R_l + R_g}{R_l + R_g - (m\alpha)^2 K_c \Delta T_g} \cdot \left(\frac{\Delta T_g}{K_g} + \frac{(m\alpha)^2 T_0 \Delta T_g}{R_l + R_g} + \varepsilon\left(m\alpha\Delta T_g\right)^2 \frac{R_l}{\left(R_l + R_g\right)^2} \right) \tag{13}$$

Inserting equation (12) and (13) into equation (11) yields a cubic equation for ΔT_g which can be solved analytically [2]. The final result is:

$$\Delta T_G = -\frac{a}{3} + 2\,\mathrm{sgn}(q)\sqrt{|p|}\cos\left(\frac{1}{3}\arccos\left(\frac{|q|}{\sqrt{|p|^3}}\right) + \frac{\pi}{3}\right) \tag{16}$$

$$q = \frac{1}{2}\left(\frac{2a^3}{27} - \frac{ab}{3} + c\right) \tag{17}$$

$$p = \frac{1}{3}\left(b - \frac{a^2}{3}\right) \tag{18}$$

$$a = -\left(R_l + R_g\right)\left(\varepsilon\frac{R_g}{R_l}\left(\frac{1}{x} + \frac{1}{y}\right) + \left(\frac{1}{x} - \frac{1}{y}\right) - \frac{R_g}{R_l}\frac{1}{y}\right) \tag{19}$$

$$b = -\left(\frac{T_1}{y} + \frac{T_0}{x}\right)\frac{\left(R_l + R_g\right)^2}{R_l} - \frac{\left(R_l + R_g\right)^3}{xyR_l}\left(\frac{K_h}{K_g} + \frac{K_c}{K_g} + 1\right) \tag{20}$$

$$c = \frac{\Delta T}{xy}\frac{\left(R_l + R_g\right)^3}{R_l} \tag{21}$$

$$x = (m\alpha)^2 K_c \tag{22}$$

$$y = (m\alpha)^2 K_h \tag{23}$$

The thermal (electrical) resistance K_g (R_g) can be expressed as:

$$K_g = \frac{1}{m\left(\frac{\lambda_n A_n}{l_n} + \frac{\lambda_p A_p}{l_p}\right)} \tag{24}$$

$$R_g = m\left(\frac{\rho_n l_n}{A_n} + \frac{\rho_p l_p}{A_p} + 2\left(r_{ch} + r_{cc}\right)\right) \tag{25}$$

where A_n (A_p) is the cross sectional area of the n-leg (p-leg), λ_i and ρ_i are the corresponding thermal and electrical resistivities, and r_{cc} (r_{ch}) is the electrical contact resistance per junction.

The result is similar to the calculation in [3]. The authors chose ε=1/2 and $R_l = R_g$ for load matching, which will be modified in the following section.[1]

Simplification

The result for ΔT_g in equation (16-23) is complicated. To simplify, we perform a Taylor expansion about $(m\alpha)^2 K_c \Delta T_g/(R+R_g)$ of equation (12) and (13). Neglecting all terms corresponding to $O(\Delta T_g^2)$ and higher we obtain:

$$q_h \approx \frac{\Delta T_g}{K_g} + \frac{(m\alpha)^2 T_1 \Delta T_g}{R_l + R_g} \approx \frac{\Delta T_g}{K_g} + \frac{(m\alpha)^2 T_0 \Delta T_g}{R_l + R_g} \tag{26}$$

$$q_c \approx \frac{\Delta T_g}{K_g} + \frac{(m\alpha)^2 T_0 \Delta T_g}{R_l + R_g} \tag{27}$$

Inserting equation (26) and (27) into (11), the temperature difference ΔT_g and P_{out} can be expressed in the following way:

$$\Delta T_g = \frac{\Delta T}{1 + \frac{K_c}{K_g} + \frac{K_h}{K_g} + \frac{T_0(x+y)}{R_l + R_g}} \tag{28}$$

[1] The choice ε=1/2 often leads to the wrong statement, that half of the Joule heat flows back to the heat source. Instead, due to the flow of an electric current accompanied by Joule heat, the temperature gradient at the heat source in the thermo couples reduces by half of the Joule heat.

$$P_{out} = (\Delta T m\alpha)^2 \left(\frac{K_g}{K_g + K_c + K_h}\right)^2 \frac{R_l}{\left(R_l + R_g^{\text{eff}}\right)^2} \qquad (29)$$

where we introduced the effective inner resistance R_g^{eff}:

$$R_g^{\text{eff}} = R_g + T_0(x+y)\frac{K_g}{K_g + K_c + K_h} \qquad (30)$$

Load Matching

To find the load impedance R_l which enables the TEG to operate at maximal output power, the equation

$$\left.\frac{d}{dR_l}P_{out}\right|_{R_l = R_{\max}} = 0 \qquad (31)$$

has to be solved. The result is

$$R_{\max} = R_g^{\text{eff}} \qquad (32)$$

which means the load resistance has to be chosen equal to an effective inner resistance. A similar result has been found in [4].

Geometry Optimization

A crucial point in designing TEGs is to determine the best generator geometry with respect to available materials and manufacturing technologies. In this paper we want to discuss this via an example to determine the optimal length l of a thermo couple, in order to optimize the generator for maximal output power. The load is matched corresponding to equation (30, 32). The electrical contact resistances are neglected. In addition, we chose $A_n = A_p = A_{tc}$. By combining equations (24-25, 29-30) and after maximizing, we get the following expression for the optimal length $l^{\max}$:

$$l^{\max} = \sqrt{\frac{(\lambda_n + \lambda_p)(\rho_n\lambda_n + \rho_p\lambda_n + \rho_n\lambda_p + \rho_p\lambda_p + T_0\alpha^2)}{\rho_n + \rho_p}} \cdot (K_c + K_h) m A_{tc} \qquad (33)$$

An example calculation is demonstrated in Figure 2, where we used the values $A_{tc} = 0.25\ \text{mm}^2$, $m = 200$, $K_h = 1.0$ K/W, and $K_c = 10$ K/W. The material properties of Bi_2Te_3 (typical at ambient temperature) are given in Table 1. The solid line is the exact solution described in equation (1-3, 16-23), the dotted line is the simplified model (equation (29)) with $l^{\max} \approx 1.29$ mm. The plus sign line is a first order model, used by many researchers (e.g. [6], [7]). Latter, $R = R_g$ is used for load matching.

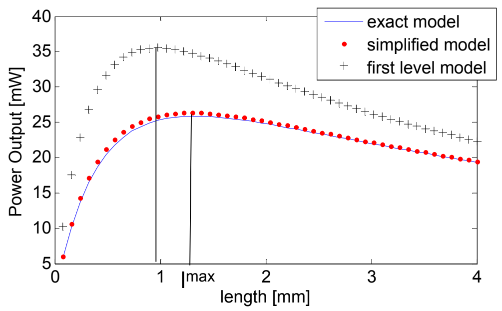

FIGURE 2: Power output vs. thermo couple length.

Material	α [µV/K]	ρ [Ωm]	λ [W/mK]
p-Bi_2Te_3	173	9.27E-6	0.963
n-Bi_2Te_3	-209	23.8E-6	0.800

TABLE 1: Thermoelectric properties of Bi_2Te_3 [5].

The observed difference is mainly due to the influence of Peltier heat. The thermodynamic limit, presented in the next section, is about $P_{out}^{\max} \approx 175$ mW.

Thermodynamic limit

In addition to comparing the efficiency of a TEG to the thermodynamic limit

$$\eta_c = \frac{\Delta T}{T_h}, \qquad (34)$$

a comparison with the physical limit of power generation is also of great interest. If the heat energy q_h is used in the most efficient way, the power output is given by:

$$P_{out} = \eta_c q_h = \frac{T_1 - T_h}{K_h}\frac{T_h - T_c}{T_h} \qquad (35)$$

Equation (35) has to be maximized under the constraint that the heat energy, which is coupled out to the heat sink, is given by:

$$q_{out} = q_c = \frac{T_c - T_0}{K_c} \qquad (36)$$

The result is:

$$P_{out}^{\max} = \frac{\left(\sqrt{T_1T_0} - T_0\right)\left(T_1 - \sqrt{T_1T_0}\right)}{\sqrt{T_1T_0}\,(K_c + K_h)} \qquad (37)$$

which can be approximated by a Taylor expansion about $\Delta T/T_1$, resulting in:

$$P_{out}^{\max} \approx \Delta T^2 \frac{1}{4T_0(K_c + K_h)} \qquad (38)$$

Note, that in addition to the best possible efficiency, there is also an optimization corresponding to the temperature difference T_h-T_c.

Measurements and Theory Comparison

To compare the power predicted by the model, we performed a measurement for typical TEGs with a size of A=16 cm^2. The TEG data are given in Table 2.

TEG	$m\alpha$ [V/K]	K_g [K/W]	R_g [Ω]	R_l [Ω]
127-150-9	0.050	2.907	3.4	4
127-150-22	0.055	1.437	1.54	2
199-150-2	0.082	0.641	1.67	2

TABLE 2: TEG data (TEGs and datasheet from [8]).

The measurements were performed at an ambient temperature of 24 °C, and the hot side temperature was varied in the range of 32-50 °C. The heat sink K_c was chosen to be $K_c \approx 6$ K/W (small temperature dependence). The results are presented in Figure (3), which shows, there is a good agreement between the calculated and the measured

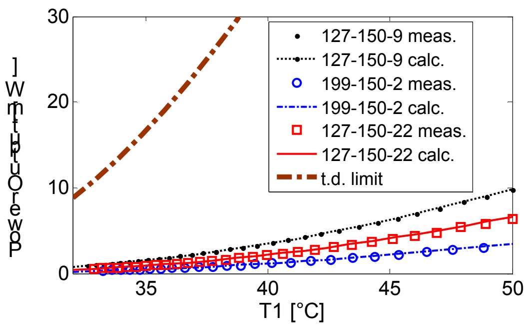

FIGURE 3: Power Output vs. heat source temperature.

data. The dashed dotted line shows the thermodynamic limit.

Comparison between different TEGs

The strong influence of the Peltier heat suggests comparing TEGs under different heat sink conditions K_c. Consequently we calculate the power output using the simplified model with matched load (equation (30, 32) as a function of the thermal conductance $1/K_c$. The results are depicted in Figure 4. There can be made 2 conclusions: 1 the power output depends strongly on K_c and 2 the curves cross each other. Notice that the last point is only due to the Peltier effect, which indicates that according to the heat sink condition, the thermoelectric properties have to be tuned properly.

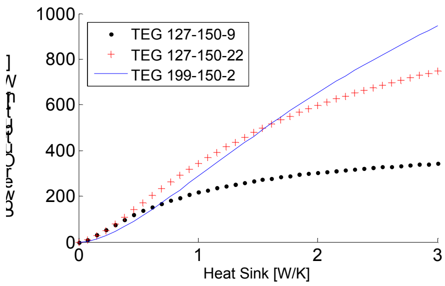

FIGURE 4: Power Output vs. $1/K_c$.

This is an essential observation for users, to be able to choose the most appropriate generator for their application.

Conclusion

A new model for TEGs was introduced, and a simplification was performed. Geometry optimization under matched load has been investigated and compared with a first order model. The thermodynamic limit for power generation was presented and compared with commercially available TEGs, which are obviously well below the theoretical limit. The TEGs are compared with each other under different heat sink conditions. The results enable one to choose the best TEG for a given heat sink.

References

1. M. H. Cobble, *"Calculations of Generator Performance"*, Handbook of Thermoelectrics, CRC Press, (1995).
2. Teubner-Taschenbuch der Mathematik, B. G. Teubner Verlagsgesellschaft Leipzig (1996).
3. M. Strasser, R. Aigner, C. Lauterbach, T.F. Sturm, M. Franosch, G. Wachutka, *"Micromachined CMOS thermoelectric generators as on-chip power supply"*, Sens. Act. A, Vol. 97-98C, pp. 535-542, (2002).
4. K. Matsuura, T. Honda, H. Kinoshita, *"Thermo-electric generation by direct heat exchange in ocean thermal energy conversion*", Technology Report of the Osaka University, Vol. 33, No., 1983, p 59, (1983).
5. Thermoelectric Handbook, Macro To Nano, ORC Press, (2006).
6. G. Min, D. M. Rowe, *"Optimisation of thermoelectric module geometry for waste heat electrical power generation*", J. Power Sources, Vol. 38, pp. 253 -259, (1991).
7. W. Glatz, S. Muntwyler, C. Hierold, *"Optimization and fabrication of thick flexible polymer based micro thermoelectric generators",* Sens. Act. A 132, pp. 337-345, (2006).
8. http://www.thermalforce.de ([Online] 29 May 2008).